Interferometer Calibration and Source Position Measurements on Baseline 2

C. M. Wade, B. G. Clark, D. E. Hogg

March 1965

I. Introduction

Numerous observations of standard calibration sources (3C 48, 3C 147, 3C 196) were made while the interferometer was operating on Baseline 2 during October 1964 to January 1965. In addition, a number of small-diameter sources were observed for the purpose of fixing their positions accurately. The present report discusses these data in detail.

The Basic Equation: The method used for calibration and position-finding was set forth in reference [1]. It depends on the behavior of the apparent visibility phase (i.e., that derived by the fringe reduction program using assumed values of the interferometer constants and the source position) of unresolved radio sources as a function of hour angle. The true visibility phase for a point source is always zero. But the apparent phase generally is not zero, and moreover it varies with hour angle. This behavior is attributable to errors in the values of B_2, h, α, and δ assumed in the reduction for phase and amplitude of the fringe pattern. It was shown in [1] that the phase as a function of hour angle is

$$\frac{1}{2\pi}\,\Phi(H) = [B_2\Delta\delta \sin\delta - \Delta B_2 \cos\delta] \cos\tau + B_2\Delta\tau \cos\delta \sin\tau + K \qquad (1)$$

(see [1] for the definitions of the terms). It is clear that errors in h and α are indistinguishable (since $\Delta\tau = -\Delta h - \Delta\alpha$) and that errors in δ and B_2 have closely related effects. Hence Δh and ΔB_2 must be found from observations of sources with precisely known positions ($\Delta\alpha = \Delta\delta = 0$). Once these are known, it is possible to find the positions of other unresolved sources accurately.

It is evident from the structure of (1) that the rate of phase change depends chiefly on the errors in δ and B_2 at low hour angles ($\tau \approx H + 7^h10^m$). In the same way, it is determined mainly by the errors in α and h at large hour angles. Thus it is essential that the observations cover a wide range of hour angles if the method is to work well. A forthcoming report by Clark will treat this point in detail. A second point to notice is that the phase behavior is very insensitive to declination errors for sources close to the equator. It is easy to show that the uncertainty in the declinations measured by our procedure varies as csc δ.

As we have implied above, this method can be used only with unresolved sources. The visibility phase changes caused by the resolution of source structure rule out objects which cannot be treated as points. Furthermore, the method relies heavily on the inherent phase stability of the instrument, since it treats all phase changes as consequences of errors in h, B_z, α and δ.

The Computer Program: Clark has written a computer program which finds $\Delta\tau$ and $J = B_z\Delta\delta \sin\delta - \Delta B_z \cos\delta$ from the observed phases by least squares, using (1) as the equation of condition. Each solution is based on the data for a single source for one observing day. With a calibration source, one has

$$\Delta h = -\Delta\tau$$
$$\Delta B_z = -J \sec\delta.$$

For other sources,

$$\Delta\alpha = -\Delta h - \Delta\tau,$$
$$\Delta\delta = (J/B_z) \csc\delta + (\Delta B_z/B_z) \operatorname{ctn}\delta.$$

The program automatically corrects the observed phases for atmospheric refraction (see [2]).

As its main output, the program gives the least squares solutions for Δh, ΔB_z, $\Delta\alpha$, and $\Delta\delta$ along with their standard deviations. It also lists alternative solutions where these are reasonably consistent with the data. A particularly useful quantity that is developed along with each solution is the r.m.s. deviation of the observed phases from those expected on the basis of that solution. This provides a direct index of the quality of the fit to the input data, and it gives one a basis for choosing the best solution when there are alternatives. Since the distribution of the observed points is an important factor in assessing the reliability of a solution, the number of points in each one-hour increment of hour angle is printed out, along with the total number of points used.

The program ignores certain data points. Those taken within 20 minutes of crossover are rejected because the early fringe reduction program used for the Baseline 2 observations is not accurate near crossover. Also rejected were those points for which the fringe reduction program found a high internal r.m.s. uncertainty.

II. Interferometer Calibration

When the calibration program for Baseline 2 was laid out, precise optical positions were available for only a few unresolved sources. We adopted 3C 48, 3C 147, 3C 196, and 3C 245. The first three of these are quasi-stellar objects whose positions had been measured by Griffin [3]. 3C 245 was identified by Hazard, Mackey, and Nicholson [4] on the strength of a lunar occultation. It was attractive as a calibrator, despite its faintness, because its declination (+12°) is much lower than those of the other three sources. We finally rejected it because it gives results which are rather discordant with those from the other sources. Another reason was the high scatter in the values it gives; these effects may be due to partial resolution (see notes following Table VI). Thus our calibration is based entirely on the three quasi-stellars.

Table I gives the mean positions from [3] for adopted calibration sources.

TABLE I

Positions of Calibration Sources [3]

Source	RA (1950.0)	Decl. (1950.0)
3C 48	$01^h\ 34^m\ 49\overset{s}{.}817$	$+32°\ 54'\ 20\overset{''}{.}22$
3C 147	$05^h\ 38^m\ 43\overset{s}{.}531$	$+49°\ 49'\ 43\overset{''}{.}11$
3C 196	$08^h\ 09^m\ 59\overset{s}{.}385$	$+48°\ 22'\ 08\overset{''}{.}03$

Correction for Local Oscillator Drift: The local oscillator frequency decreased slowly during the observing period because of the aging of the crystal. It was measured several times each day.

Since

$$B_2 = \frac{D}{\lambda} \cos d = \frac{\nu D \cos d}{c} ,$$

the value of B_2 changes according to the L.O. frequency:

$$\Delta B_2 = \frac{D \cos d}{c} \Delta\nu = B_2 \frac{\Delta\nu}{\nu} .$$

If $\Delta\nu$ is expressed in khz, we have for Baseline 2,

$$\Delta B_2 = 4.637 \times 10^{-3} \Delta\nu.$$

Table II gives the adopted local oscillator frequency for each observing day on Baseline 2. The mean frequency up to December 23 was 2694.9837 Mhz. We take this to be our standard frequency, and we shall adjust all frequency-dependent quantities to it. The table also lists the correction B_2 requires each day owing to the oscillator drift.

TABLE II
Local Oscillator Frequency and Errors in B_2 due to L.O. Drift

Date	Tape	ν_{LO} (Mhz)	ΔB_2
2-3 Nov 64	20	2694.9941	-0.048
3-4 " "	21	.9924	.040
4-5 " "	22	.9996	.074
5-6 " "	23	.9970	.061
6-7 " "	24	.9959	.057
7-8 " "	25	.9951	.053
8 " "	26	.9944	.050
8-9 " "	27	.9935	.046
9-10 " "	28	.9931	.044
10-11 " "	29	.9920	.039
13-14 " "	30	.9898	.028
14-15 " "	31	.9895	.027
15-16 " "	32	.9886	.023
16-17 " "	33	.9881	.020
17-18 " "	34	.9875	.018
18-19 " "	35	.9876	.018
19-20 " "	36	.9871	.016
20-21 " "	37	.9866	.013
21-22 " "	38	.9864	.013
22-23 " "	39	.9860	.011
24 " "	40	.9856	.009
24-25 " "	41	.9851	-0.006
1-2 Dec 64	42	.9824	+0.006
4-5 " "	43	.9812	.012
5-6 " "	44	.9811	.012
6-7 " "	45	.9811	.012
8-9 " "	46	.9800	.017
9-10 " "	47	.9800	.017
10-11 " "	48	.9796	.019
11-12 " "	49	.9791	.021
12 " "	50	.9789	.022
13-14 " "	51	.9787	.023
14 " "	52	.9784	.025
16 " "	56	.9782	.026
16-17 " "	57	.9781	.026
17-18 " "	58	.9773	.030
18-19 " "	59	.9770	.031
20 " "	60	.9769	.032
21 " "	61	.9767	.033
22-23 " "	62	.9764	.034
23-24 " "	63	.9756	.038
26-27 " "	64	.9749	.041
27-28 " "	65	.9747	.042
28-29 " "	66	.9745	.043
29-30 " "	67	.9744	.043
30-31 " "	68	.9742	.044
31 " "	69	.9739	.045
31 " " } 1 Jan 65 }	70	.9739	.045
1-2 " "	71	.9734	.048
3-4 " "	72	.9734	+0.048

The Individual Calibration Measurements: Tables IIIa-c give the individual determinations of B_λ and h for each of the three calibration sources. We have included only the cases where the r.m.s. phase difference between the input data and the computed solution is less than 10°. The B_λ values have been corrected for the local oscillator drift. Each determination has with it the internal standard deviation.

Figures 1 and 2 show the frequency distributions of B_λ and h, respectively.

TABLE IIIa

Calibration Measurements on 3C 48

Tape	B_λ		$h + 12^h$	
20	12493.465 ±	0.006	$4^h\ 49^m\ 40^s.786$ ±	$0^s.007$
21	.510	.004	.734	.006
22	.503	.002	.747	.004
29	.437	.010	.941	.017
34	.585	.002	.773	.007
41*	.492	.012	.823	.019
43	.672	.010	.663	.011
45	.547	.002	.812	.005
46	.498	.003	.874	.005
57	.554	.001	.769	.004
60	.509	.004	.830	.008
61	.539	.002	.799	.005
70	.552	.002	.700	.006
71	.559	.002	.710	.008

*Hour angle range less than 6^h.

TABLE IIIb

Calibration Measurements on 3C 147

Tape	B_λ		$h + 12^h$	
20	12493.524 ±	0.003	$4^h\ 49^m\ 40^s.745$ ±	$0^s.005$
21	.514	.006	.777	.010
22	.450	.006	.897	.010
23	.543	.004	.869	.009
24	.529	.001	.740	.002
25	.539	.001	.792	.003
31	.543	.001	.772	.003
32	.580	.002	.684	.006
44	.584	.001	.780	.003
46	.562	.002	.749	.005
47	.557	.001	.750	.003
48	.551	.002	.777	.009
49	.588	.002	.681	.007
50	.506	.002	.634	.014
65	.546	.003	.803	.007
66	.539	.002	.746	.004
67	.530	.003	.804	.007
72	.559	.002	.842	.005

TABLE IIIc

Calibration Measurements on 3C 196

Tape	B_2	$h + 12^h$
30	12493.618 ± 0.008	$4^h\ 49^m\ 40^s.766 \pm 0^s.008$
34	.629 .007	.758 .013
35	.659 .006	.725 .014
43	.524 .007	.908 .008

The Mean Values of B_2 and h: The mean values of B_2 and $h + 12^h$ are given below, with the standard deviations derived from the scatter between the individual determinations.

3C 48: The means of all 14 measurements are

$$B_2 = 12493.531 \pm 0.014$$
$$h + 12^h = 4^h\ 49^m\ 40^s.783 \pm 0^s.020.$$

The internal errors are appreciably higher for tapes 29, 41, and 43 than for the other tapes. The means for the 11 best tapes are

$$B_2 = 12493.530 \pm 0.011$$
$$h + 12^h = 4^h\ 49^m\ 40^s.776 \pm 0^s.016.$$

3C 147: The means of all 18 measurements are

$$B_2 = 12493.541 \pm 0.008$$
$$h + 12^h = 4^h\ 49^m\ 40^s.769 \pm 0^s.015.$$

The internal errors are highest in tapes 21, 22, and 50. The means for the remaining 15 tapes are

$$B_2 = 12493.552 \pm 0.005$$
$$h + 12^h = 4^h\ 49^m\ 40^s.769 \pm 0^s.013.$$

3C 196: The means of the 4 measurements are

$$B_2 = 12493.608 \pm 0.034$$
$$h + 12^h = 4^h\ 49^m\ 40^s.789 \pm 0^s.046.$$

The individual determinations for 3C 196 have higher internal uncertainties than the majority of those for 3C 48 and 3C 147. If we base our mean on the best 11 solutions for 3C 48 and the best 15 for 3C 147, we get

$$B_2 = 12493.544 \pm 0.005$$
$$h + 12^h = 4^h\ 49^m\ 40^s.772 \pm 0^s.007$$

These are the values we adopt as the final solutions for Baseline 2.

For comparison, it is interesting to note that, had we taken the average of all 36 measurements in Tables IIIa-c, we would have had

$$B_2 = 12493.545 \pm 0.006$$
$$h + 12^h = 4^h\ 49^m\ 40^s.777 \pm 0^s.009$$

Consistency between Calibration Sources: The scatter seen in Figures 1 and 2 indicates that the differences in the values of B_2 and h derived for the three calibrators separately are unlikely to be significant. Nevertheless, they deserve discussion because they may reflect (1) errors in the adopted standard positions, or (2) a variation in the effective baseline constants with declination.

There is no evidence in the present material for latter possibility. The most discordant source, 3C 196, is less than 2° south of 3C 147, which is the best observed of the three. On the other hand, 3C 48 and 3C 147 agree very closely despite a difference of nearly 18° in declination.

The possibility of real errors in the optical positions of the calibrators can not be ignored, however. Let us assume for the moment that Griffin's position for 3C 147 is perfect, and see what this implies about the locations of 3C 48 and 3C 196. We do this by interpreting the differences in B_2 and h in terms of equivalent positional shifts:

3C 48: $\Delta\alpha = -0^s.007 \pm 0^s.020$, $\Delta\delta = +0''.56 \pm 0''.38$.

3C 196: $\Delta\alpha = -0^s.020 \pm 0^s.048$, $\Delta\delta = +0''.82 \pm 0''.51$.

The agreement with Table I is fully consistent with Griffin's opinion that his determinations are accurate to within 0''.3 - 0''.5. It is still quite possible that the small differences in the calibration constants are due partly to slight errors in the adopted optical positions.

III. Source Position Measurements

Twenty-five sources were observed for the purpose of finding their positions. These were chosen because of their supposed small angular sizes. As it turned out, 3C 47 and 3C 225 were resolved. The results for four more (3C 228, 3C 263, 3C 299, 3C 433) were unusable for one reason or another. We succeeded in finding positions for the remaining 19 sources.

Position Corrections: The original data tapes were reduced with one of two sets of assumed baseline constants. These are listed in Table IV along with the corresponding corrections required for the positions found by the computer program. The values of ΔB_2 in the declination correction are to be taken from Table II.

TABLE IV

Baseline Constants Assumed in the Original Reductions

Tapes	B_2	$h + 12^h$	$\Delta\alpha$	$\Delta\delta$
20-26, 28-43, 45-47	12493.640	$4^h\ 49^m\ 41\overset{s}{.}360$	$+0\overset{s}{.}588$	$-206265'' \dfrac{(0.096+\Delta B_2)}{B_2} \text{ ctn } \delta$
27,44, 48-72	12493.600	$4^h\ 49^m\ 40\overset{s}{.}760$	$-0\overset{s}{.}012$	$-206265'' \dfrac{(0.056+\Delta B_2)}{B_2} \text{ ctn } \delta$

The Individual Position Measurements: The corrected individual position measurements are given in Table V. The table includes the internal r.m.s. uncertainties of the solutions. The column headed "Quality Code" gives certain information which bears on the reliability of the solution. The meanings of the symbols are as follows:

Code Symbol	Significance
0	R.m.s. phase deviation less than 10°
*	" " " between 10° and 20°
**	" " " greater than 20°
†	Computer program found alternative solutions
X	Observations covered less than 6^h of hour angle.

Solutions with code 0 are generally good; those with * are somewhat suspect except for the weakest sources; and those with ** are likely to be worthless. The alternative solutions for the cases listed in Table V are invariably much worse than the solution given.

TABLE V

Corrected Individual Position Measurements

Source	Tape	RA(1950.0)	Std. dev.	Decl.(1950.0)	Std. dev.	Quality Code
CTA 21	35	$3^h\ 16^m\ 09^s.124$	$0^s.017$	$+16°\ 17'\ 39''.34$	$0''.36$	0X
	36	09.191	.031	40.29	0.66	0X
	39	08.971	.062	30.31	1.35	*†X
3C 84	64	$3^h\ 16^m\ 29^s.611$	$0^s.011$	$+41°\ 19'\ 51''.34$	$0''.05$	0
	65	.587	.008	50.92	.04	0
	66	.603	.003	51.66	.02	0
	67	.634	.004	51.18	.03	0
3C 91	41	$3^h\ 34^m\ 03^s.789$	$0^s.083$	$+50°\ 36'\ 05''.87$	$0''.33$	*†X
3C 119	28	$4^h\ 29^m\ 07^s.588$	$0^s.009$	$+41°\ 32'\ 08''.49$	$0''.03$	0
	29	.822	.013	08.19	.04	0
	33	.941	.036	06.69	.13	*†
	34	.879	.016	07.62	.05	0
3C 138	28	$5^h\ 18^m\ 16^s.291$	$0^s.012$	$+16°\ 35'\ 28''.41$	$0''.19$	0
	29	.437	.011	27.39	.14	0
	33	.544	.031	25.83	.55	0†
	34	.466	.013	25.22	.18	0†
3C 158	40	$6^h\ 18^m\ 50^s.255$	$0^s.613$	$+14°\ 33'\ 42''.31$	$12''.65$	*†X
	41	.077	.106	41.73	0.72	*†X
3C 216	32	$9^h\ 06^m\ 17^s.349$	$0^s.013$	$+43°\ 05'\ 58''.34$	$0''.20$	0
	45	.363	.010	60.43	.14	0
	46	.291	.018	58.89	.29	0
3C 237	35	$10^h\ 05^m\ 22^s.099$	$0^s.013$	$+\ 7°\ 44'\ 58''.79$	$0''.56$	0†
	36	21.977	.018	55.12	0.85	0†
	38	22.190	.138	58.00	2.19	0X
	39	22.146	.068	60.45	4.46	0†X
3C 245	20	$10^h\ 40^m\ 06^s.034$	$0^s.013$	$+12°\ 19'\ 12''.99$	$0''.47$	0†
	21	06.033	.020	12.62	0.87	*†
	26	06.102	.033	14.84	3.91	0X
	29	06.220	.059	24.82	3.36	*†X
	31	06.221	.017	19.43	0.53	*†
	44	06.033	.009	14.89	0.31	0†
	47	06.135	.009	12.40	0.52	0†
	48	05.730	.126	18' 55.47	6.37	0X
	50	05.929	.073	67.90	3.10	0X
	51	05.530	.102	58.52	4.32	0X
	68	05.814	.111	59.14	4.52	0X

TABLE V, (continued)
Corrected Individual Position Measurements

Source	Tape	RA(1950.0)	Std. dev.	Decl.(1950.0)	Std. dev.	Quality Code
3C 286	28	$13^h\ 28^m\ 50^s.014$	$0^s.066$	$+30°\ 45'\ 58''.94$	$0''.25$	0X
	29	49.581	.034	57.52	.16	0†
	33	49.622	.023	55.89	.12	0
	34	49.601	.019	58.96	.09	0
	56	49.515	.007	59.96	.06	0
	58	49.476	.010	58.04	.08	0†
	60	49.739	.006	58.45	.04	0
	61	49.708	.010	58.61	.07	0
	62	49.693	.012	59.33	.11	0†
	70	49.610	.005	58.35	.05	0
	72	49.501	.053	60.49	.24	0X
3C 287	35	$13^h\ 28^m\ 16^s.078$	$0^s.026$	$+25°\ 24'\ 38''.24$	$0''.42$	0X
	36	15.921	.059	38.16	1.23	0†X
	39	16.382	.051	42.92	0.68	0X
3C 295	40	$14^h\ 09^m\ 33^s.469$	$0^s.010$	$+52°\ 26'\ 12''.16$	$0''.02$	0
3C 298	27	$14^h\ 16^m\ 28^s.777$	$0^s.014$	$+\ 6°\ 42'\ 13''.73$	$0''.74$	0
	33	.645	.029	00.78	1.75	0†
	34	.736	.025	13.88	1.43	0†
3C 318	35	$15^h\ 17^m\ 53^s.102$	$0^s.370$	$+20°\ 28'\ 45''.44$	$9''.43$	**†X
	36	50.642	.093	26' 47.70	2.32	0†X
	39	50.630	.091	26' 50.76	2.32	0†X
3C 345	27	$16^h\ 41^m\ 17^s.568$	$0^s.013$	$+39°\ 54'\ 10''.20$	$0''.15$	0
	32	.511	.016	09.31	0.19	0
	33	.352	.122	10.86	1.23	**†
	34	.675	.016	11.26	0.19	0
3C 380	21	$18^h\ 28^m\ 13^s.423$	$0^s.012$	$+48°\ 42'\ 40''.62$	$0''.19$	0X
	22	.394	.006	39.82	.06	0
	24	.516	.014	41.23	.32	0
	26	.447	.007	40.03	.08	0
	30	.546	.006	40.78	.07	0
	32	.345	.028	39.86	.12	0†
	33	.305	.018	39.45	.06	0†
	34	.456	.015	40.24	.05	0†
	35	.360	.010	40.35	.03	0
	36	.473	.014	38.62	.04	0
	39	.321	.009	39.77	.02	0
	40	.372	.009	38.45	.04	0†
	43	.543	.005	40.59	.05	0
	44	.484	.032	39.56	.10	0X
	47	.414	.007	37.89	0.13	0X

TABLE V, (continued)
Corrected Individual Position Measurements

Source	Tape	RA(1950.0)	Std. dev.	Decl.(1950.0)	Std. dev.	Quality Code
3C 380 (cont'd)	49	.419	.009	40.49	.04	0†
	50	.666	.012	39.77	.04	0†
	51	.555	.011	39.62	.03	0†
	64	.530	.014	40.69	.06	0†
	65	.548	.015	40.15	.07	0†
	66	.675	.010	39.74	.04	0
	67	.475	.009	39.77	.03	0
	68	.554	.012	40.24	.05	0†
	72	.376	.044	40.78	.29	0X
3C 409	32	$20^h\ 12^m\ 18^s.110$	$0^s.034$	+23° 25' 43".21	0".66	0†X
	33	17.936	.025	40.32	.49	0
	34	18.007	.017	41.61	.34	0X
CTA 102	35	$22^h\ 30^m\ 07^s.685$	$0^s.033$	+11° 28' 23".25	0".52	0X
	36	.229	.028	25.67	.44	0X
	38	.723	.017	20.47	.34	0X
	39	.521	.022	25.94	.36	0X
3C 459	40	$23^h\ 14^m\ 02^s.202$	$0^s.048$	+ 3° 49' 06".00	1".69	0†

<u>Mean Source Positions:</u> Table VI gives the averaged positions from Table V, along with their standard deviations as derived from the scatter between the individual measurements. Comments for most of the sources follow the table.

TABLE VI
Averaged Source Positions

Source	RA(1950.0)	Decl.(1950.0)	No. of Tapes	Notes
CTA 21	$3^h\ 16^m\ 09^s.158 \pm 0^s.035$	+16° 17' 39".82 ± 0".50	2	x
3C 84	$3^h\ 16^m\ 29^s.609 \pm 0^s.012$	+41° 19' 51".28 ± 0".19	4	
3C 91	$3^h\ 34^m\ 02^s.789$	+50° 36' 05".87	1	x
3C 119	$4^h\ 29^m\ 07^s.763 \pm 0^s.097$	+41° 32' 08".10 ± 0".29	3	x
3C 138	$5^h\ 18^m\ 16^s.435 \pm 0^s.063$	+16° 35' 26".71 ± 0".80	4	x
3C 158	$6^h\ 18^m\ 50^s.077$	+14° 33' 41".73	1	x
3C 216	$9^h\ 06^m\ 17^s.334 \pm 0^s.024$	+43° 05' 59".22 ± 0".70	3	
3C 237	$10^h\ 05^m\ 22^s.038 \pm 0^s.061$	+ 7° 44' 56".96 ± 1".84	2	x
3C 245	$10^h\ 40^m\ 06^s.091 \pm 0^s.038$	+12° 19' 44".47 ± 1".41	5	x
3C 286	$13^h\ 28^m\ 49^s.642 \pm 0^s.049$	+30° 45' 58".59 ± 0".42	11	
3C 287	$13^h\ 28^m\ 16^s.127 \pm 0^s.113$	+25° 24' 39".77 ± 1".19	3	
3C 295	$14^h\ 09^m\ 33^s.469$	+52° 26' 12".16	1	x
3C 298	$14^h\ 16^m\ 38^s.719 \pm 0^s.044$	+ 6° 42' 09".46 ± 4".37	3	x
3C 318	$15^h\ 17^m\ 50^s.636$	+20° 26' 49".23 ± 1".53	2	x
3C 345	$16^h\ 41^m\ 17^s.581 \pm 0^s.055$	+39° 54' 10".26 ± 0".65	3	x
3C 380	$18^h\ 28^m\ 13^s.464 \pm 0^s.015$	+48° 42' 39".98 ± 0".13	25	
3C 409	$20^h\ 12^m\ 18^s.018 \pm 0^s.058$	+23° 25' 41".71 ± 0".96	3	
CTA 102	$22^h\ 30^m\ 07^s.540 \pm 0^s.124$	+11° 28' 23".83 ± 1".37	4	x
3C 459	$23^h\ 14^m\ 02^s.202$	+ 3° 49' 06".00	1	x

CTA 21: Result based on Tapes 35 and 36. Tape 39 was rejected because of its much lower quality. It should be noted that the hour angle coverage was under 6^h in all these observations. No very large hour angles were included, so the right ascension may not be reliable.

3C 91: This is a doubtful result since it is based on a single observation, gives a fairly high r.m.s. phase deviation, and covers a relatively small hour angle range. The observations are all at low hour angles, so the right ascension is especially untrustworthy.

3C 119: Based on Tapes 28, 29, and 34. Tape 33 was rejected because of its relatively poor quality.

3C 138: Omitting Tape 33, the poorest of the four, one gets

$$5^h\ 18^m\ 16\overset{s}{.}398 \pm 0\overset{s}{.}058,\ +16°\ 35'\ 27\overset{''}{.}01 \pm 1\overset{''}{.}06.$$

3C 158: Based on Tape 41 only. The same comments as for 3C 91 apply here.

3C 237: Based on the two best tapes, 35 and 36. The solution would be

$$10^h\ 05^m\ 22\overset{s}{.}103 \pm 0.054,\ +7°\ 44'\ 58\overset{''}{.}09 \pm 1\overset{''}{.}33$$

if all four tapes were used. The declination is small enough that it is not fully reliable.

3C 245: Based on Tapes 20, 21, 31, 44, and 47, which have the best hour angle coverage and the lowest internal r.m.s. deviations. It is interesting to note that Tapes 48, 50, 51, and 68, which have a lopsided hour angle coverage concentrated to the west of the meridian, give right ascensions and declinations which are systematically lower than those obtained with full hour angle coverage. On the other hand, Tapes 26 and 29, which include still greater west hour angles, give higher right ascensions and declinations. This probably indicates that the source is being resolved. Therefore the position given in the table should not be trusted.

3C 295: While this is based on a single solution, it is of very good quality.

3C 298: The proximity of the source to the equator probably accounts for the high scatter in the declinations.

3C 318: Based on Tapes 36 and 39. The hour angle coverage is poor. The declination given is much more reliable than the right ascension.

3C 345: Based on Tapes 27, 32, and 34.

CTA 102: The hour angle coverage is heavily concentrated to the east in all four observations. The result given is probably reliable nevertheless.

3C 459: The declination is very uncertain because the source is so close to the equator.

The standard deviations given include no allowance for the further uncertainty of $\pm 0^s.007$ and $\pm 0''.08 \csc \delta$ in right ascension and declination respectively, owing to the possible errors in h and B_ℓ.

Comparison with Optical Positions: Accurate optical positions are now available for a number of the sources in Table VI. These are given in Table VII along with the differences from our positions in each coordinate.

TABLE VII

Comparison with Optical Positions

Source	Optical Position (1950.0)		Ref.	Radio - Optical	
	R.A.	Decl.		Δα	Δδ
3C 84	$3^h\ 16^m\ 29^s.4$	$+41°\ 19'\ 52''$	5	$+0^s.2 \pm 0^s.01$	$-1'' \pm 0''.2$
3C 119	$4^h\ 29^m\ 07^s.84$	$+41°\ 32'\ 08''.7$	6	$-0^s.08 \pm 0^s.10$	$-0''.6 \pm 0''.3$
3C 216	$9^h\ 06^m\ 17^s.26$	$+43°\ 05'\ 59''.0$	6	$+0^s.07 \pm 0^s.03$	$+0''.2 \pm 0''.7$
3C 245	$10^h\ 40^m\ 06^s.00$	$+12°\ 19'\ 17''.9$	4	$+0^s.09 \pm 0^s.04$	$-3''.4 \pm 1''.4$
3C 286	$13^h\ 28^m\ 49^s.74$	$+30°\ 45'\ 59''.3$	6	$-0^s.10 \pm 0^s.05$	$-0''.7 \pm 0''.4$
3C 287	$13^h\ 28^m\ 16^s.12$	$+25°\ 24'\ 37''.1$	6	$+0^s.01 \pm 0^s.11$	$+2''.7 \pm 1''.2$
3C 295	$14^h\ 09^m\ 33^s.44$	$+52°\ 26'\ 13''.6$	3	$+0^s.03$	$-1''.4$
3C 298	$14^h\ 16^m\ 38^s.82$	$+\ 6°\ 42'\ 21''.6$	3	$-0^s.10 \pm 0^s.05$	$-12''.1 \pm 4''.4$
3C 345	$16^h\ 41^m\ 17^s.70$	$+39°\ 54'\ 11''.1$	6	$-0^s.12 \pm 0^s.06$	$-0''.8 \pm 0''.7$
3C 380	$18^h\ 28^m\ 13^s.38$	$+48°\ 42'\ 39''.3$	6	$+0^s.08 \pm 0^s.02$	$+0''.7 \pm 0''.2$
CTA 102	$22^h\ 30^m\ 07^s.71$	$+11°\ 28'\ 22''.8$	6	$-0^s.17 \pm 0^s.13$	$+1''.0 \pm 1''.4$
3C 459	$23^h\ 14^m\ 02^s.6$	$+\ 3°\ 48'\ 57''$	5	$-0^s.4$	$+9''$

The agreement between the radio and optical positions is generally good. The largest discrepancies occur near the equator, where our method is relatively insensitive to the source declination.

Figures 3 and 4 show how the differences between the radio and optical positions in the two coordinates are distributed in declination. Vertical bars show the standard deviations. There appears to be no systematic correlation, greater than $1''.5$, with declination in either coordinate. The most discordant right ascension is that of 3C 459, which depends on a single poor solution. The declination scatter increases toward the equator, as we expected.

Two important conclusions can be drawn from Figures 3 and 4:

1. The baseline parameters are not functions of declination. B_2 (and hence B_1) and h can be regarded as true constants of the instrument. A related conclusion is that the allowance we have made for atmospheric refraction must be very nearly correct.

2. The radio source identifications underlying the optical positions in Table VII must be correct. The high consistency between the radio and optical positions would be impossible if this were not true.

In closing, another point must be made. The internal standard deviations of the individual solutions are much smaller than one would expect from the differences between separate solutions. This indicates that there must be systematic effects of some kind which vary from day to day. These may be due to instrumental variations (for example, slow changes in B_3 during each day's run) or to atmospheric effects. It is important that we try to understand what the causes are and eliminate them if possible. Otherwise we shall not be using the instrumental capabilities fully.

References

1. Wade, C. M., "Interferometer Calibration and Source Position Measurement Using Long-Run Phase Behavior", NRAO Report, December, 1964.

2. Clark, B. G., "Refraction", NRAO Report, December, 1964.

3. Griffin, R. F., A.J. 68, 421, 1963.

4. Hazard, C., Mackey, M. B., and Nicholson, W., Nature 202, 227, 1964.

5. Matthews, T. A. Private communication.

6. Veron, P. Quoted in letter from Sandage to Heeschen, January 1965.

Frequency Distribution of $h + 12^h$

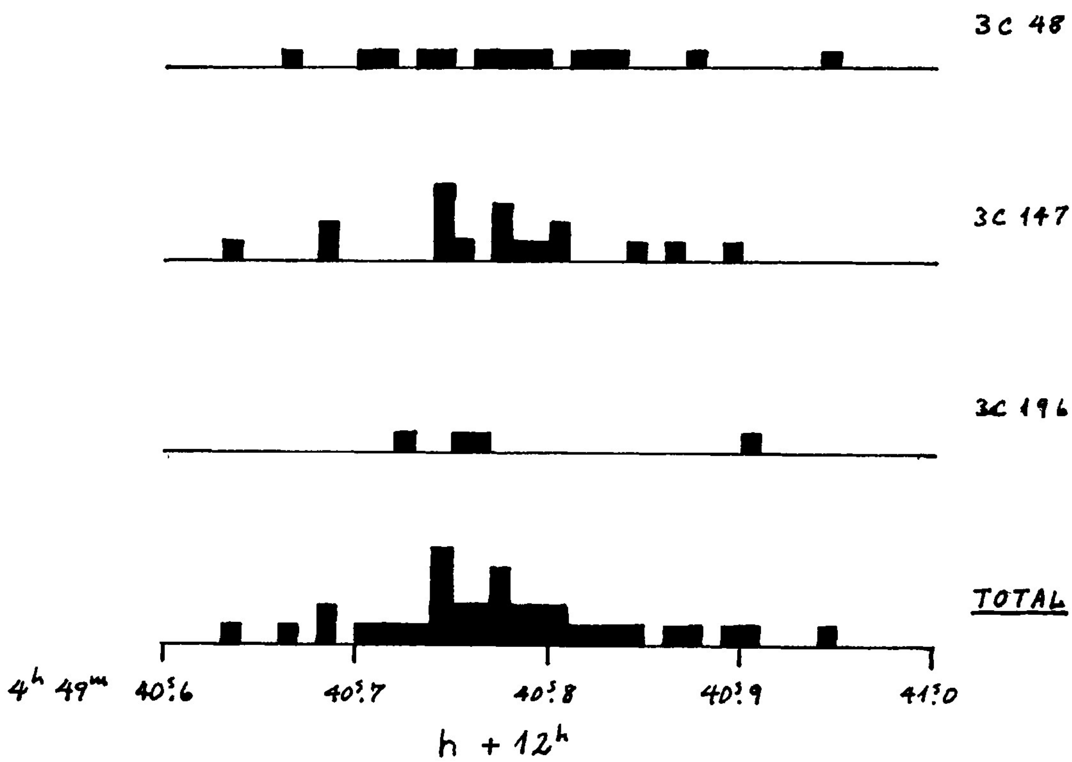

Figure 1.

Frequency Distribution of B_2

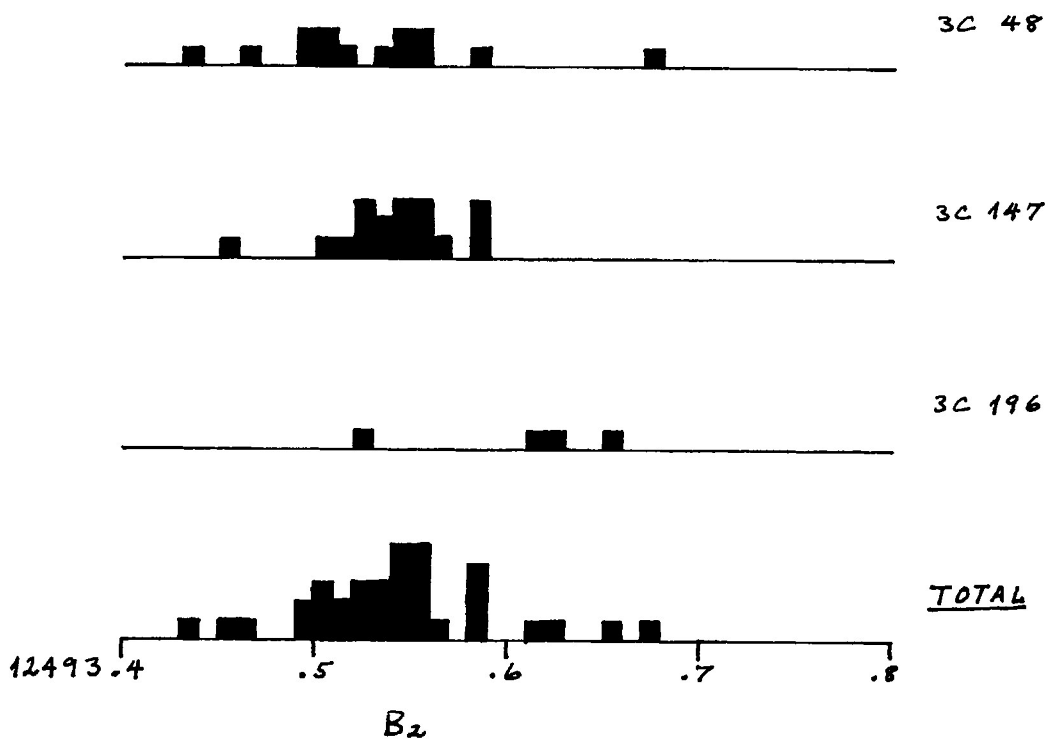

Figure 2.

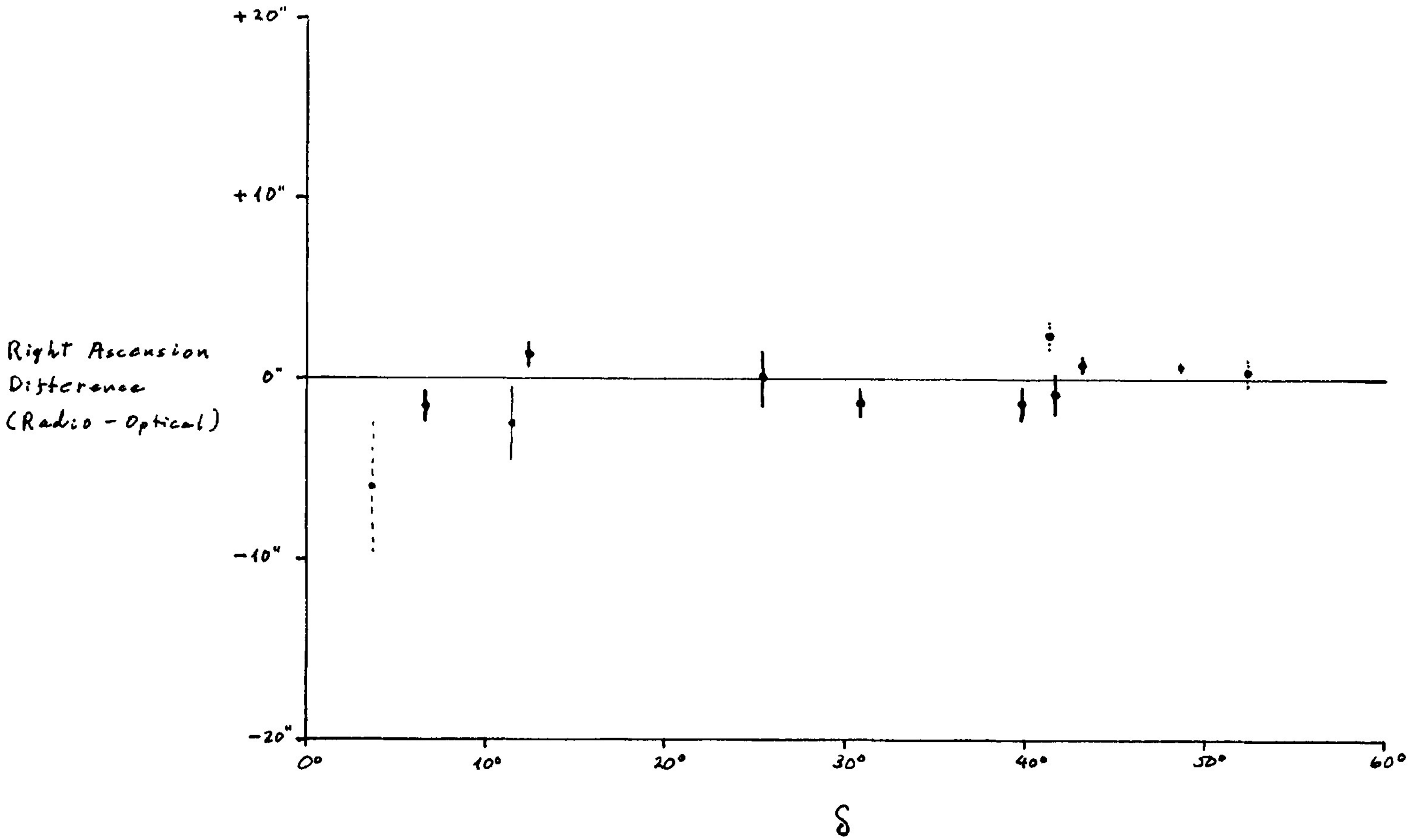
+20"
+10"
0"
-10"
-20"
Right Ascension
Difference
(Radio - Optical)
0°
10°
20°
30°
40°
50°
60°
δ

Figure 3

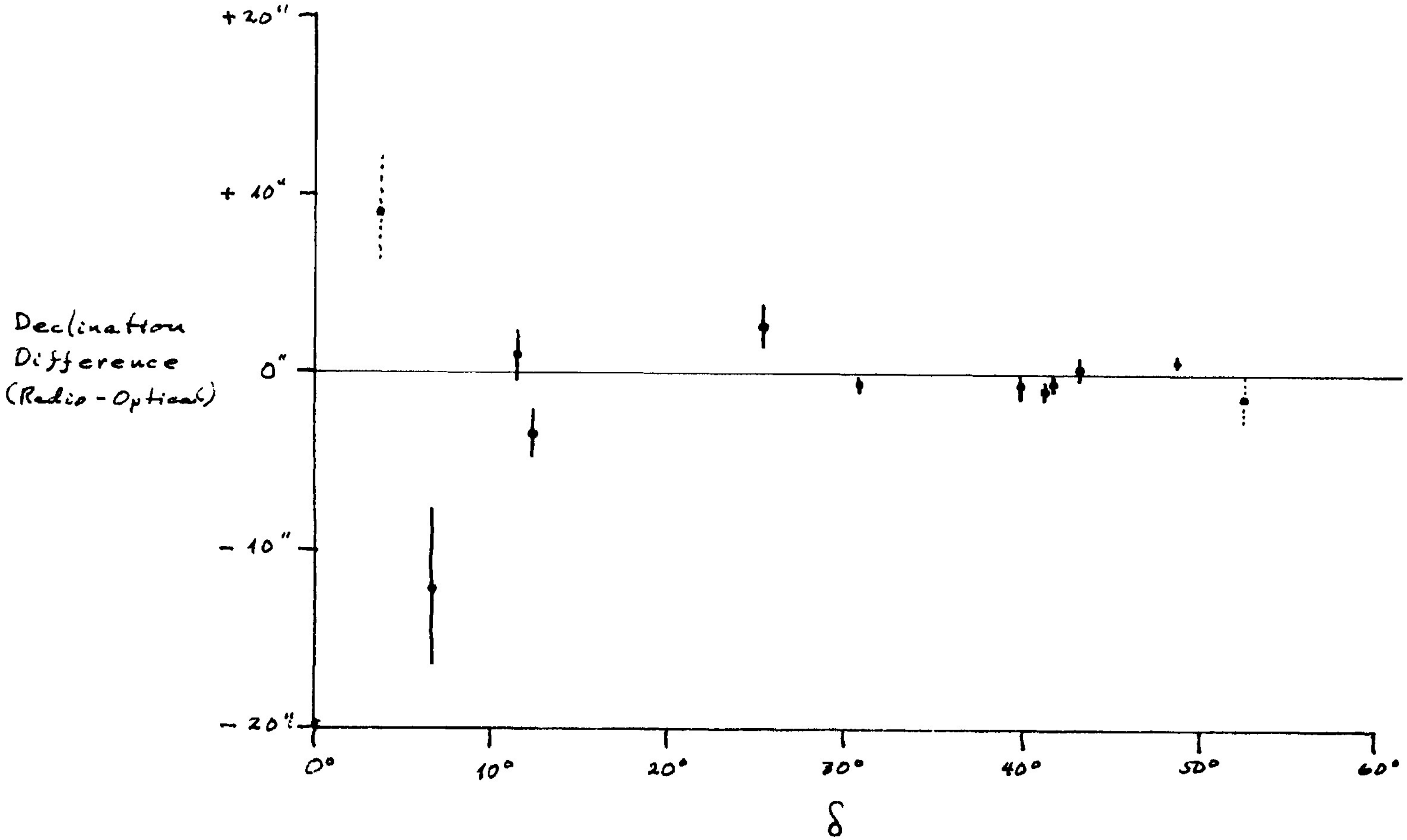
+20"
+10"
0"
-10"
-20"
Declination
Difference
(Radio - Optical)
0°
10°
20°
30°
40°
50°
60°
δ

Figure 4